




The Variability and Radial Velocity of Planetary Nebula Central Stars

A. Ali¹  and A. Mindil²

¹ Astronomy, Space Science & Meteorology Department, Faculty of Science, Cairo University, Giza 12613, Egypt; afouad@sci.cu.edu.eg

² Department of Physics, College of Science, University of Jeddah, Jeddah, Saudi Arabia; amindil@uj.edu.sa

Received 2022 September 1; revised 2023 January 2; accepted 2023 February 15; published 2023 March 24

Abstract

The extremely accurate estimates of stellar variability and radial velocity in the Gaia Data Release 3 (Gaia DR3) have enabled us to examine the close binarity and radial velocity (RV) of central stars (CSs) of planetary nebulae (PNe). This study is twofold: (1) searching for new close binary CS candidates to better understand how binarity affects the formation and evolution of PNe; and (2) extending the sample size of known RVs of PNe in order to understand their kinematics and the dynamics of the Milky Way. As a target sample, we used all true, possible, and likely PNe available in the literature. Then, we looked for their matched Gaia DR3 sources that provide measurements of variability and RV. As a result, we detected the first large collection of trustworthy photometric variability of 26 symbiotic stars and 82 CSs. In this CS group, there are 24 sources already classified as true close binary CSs in the literature. Hence, we discovered 58 new close binary CS candidates. This close binary (CB) sample represents more than half of what is currently available in the literature. In addition, we identified the radial velocities for 51 PNe. To our knowledge, 24 of these were measured for the first time. The RV measurements predicted by Gaia, based on the Doppler shift of the CS absorption lines, and those derived from nebular emission lines, show satisfactory agreement except for a few extremely high-velocity PNe.

Key words: (ISM:) planetary nebulae: general – stars: variables: general – (stars:) binaries: eclipsing – (stars:) binaries: symbiotic – techniques: radial velocities

1. Introduction

Gaia is an ESA project that aims to create a 3D representation of the Milky Way Galaxy. The Gaia Data Release 1 (Gaia DR1) appeared in 2016 September. This was followed by Gaia Data Release 2 (Gaia DR2) in 2018 April and Early Data Release 3 (Gaia EDR3) in 2020 December. The Gaia DR3 was published on 2022 June 13. It provides positions and apparent magnitudes of ~ 1.8 billion sources, as well as parallaxes, proper motions, and colors of ~ 1.5 billion objects. In comparison to Gaia DR2, Gaia DR3 exhibits significant improvements in astrometric and photometric accuracy, precision, and homogeneity. In addition to updating earlier releases, Gaia DR3 contains new data, such as astrophysical parameters (Creevey et al. 2022), BP/RP spectra (De Angeli et al. 2022), and variability classification (Eyer et al. 2022). According to Eyer et al. (2022), Gaia DR1 has ~ 3000 variable sources, Gaia DR2 has $\sim 550,000$ variable sources, and Gaia DR3 has ~ 10.5 million variable sources.

The topic of binarity has important implications for our understanding of cataclysmic variables and novae, type Ia supernovae, symbiotic stars (SySts), and other phenomena such as the production of astrophysical jets (Boffin & Jones 2019). Binary interactions occur between stars of all sizes and orbital separations, ranging from compact white dwarfs with 5-minute orbital periods to giant stars with hundred-year orbital periods.

From an observational and theoretical perspective, all stars with masses ranging from 1 to 8 solar masses, roughly 95% of the Galaxy's stellar population, will undergo the planetary nebula (PN) stage of evolution. As a consequence, studying the binary CSs of PNe is crucial to our understanding of many astrophysical phenomena that have traditionally been attributed to single-star evolution (Aller et al. 2020).

The Hong Kong/AAO/Strasbourg H α (HASH) catalog (Parker et al. 2016) contains ~ 3500 PNe, with 80% displaying complex morphologies that differ from sphericity, such as elliptical, bipolar, and multipolar PNe, as well as various internal features such as multi-shells, jets, and knots. Currently, there is widespread agreement on the importance of central star (CS) binarity in understanding PN divergence from sphericity, where the various morphologies of PNe can no longer be explained by single-star models. Since the number of detected binary CSs has increased significantly over the past decade, it has become obvious that the wide variety of PN morphologies and some of the associated unusual chemical properties are the products of binary evolution. A common-envelope event is the best method for generating an axisymmetric PN via binary interaction. The close binary (CB) fraction is the most rigorous binarity test in PN formation. Despite the challenge of finding CS infrared excesses, De Marco et al. (2013) successfully employed the technique to calculate a binary fraction, obtaining

Table 2
The Variable SySts in Gaia DR3

#	target_id	l	b	Gaia DR3 Designation	G	$B-R$	Type
1	PN ShWi 5	1.21	-3.90	Gaia DR3 4050209822908746240	15.3	1.2	Symbiotic Star
2	PN H 1-45	2.02	-2.06	Gaia DR3 4062646712567004416	14.3	3.0	Symbiotic Star
3	PN Ap 1-11	3.12	-4.63	Gaia DR3 4050848540419995776	13.2	3.1	Symbiotic Star
4	PN H 2-43	3.49	-4.87	Gaia DR3 4050670827750135040	13.6	1.2	Symbiotic Star
5	IRAS 17554-2628	3.58	-1.22	Gaia DR3 4064034330564300928	19.8	2.8	Symbiotic Star
6	PN M 3-18	7.57	1.44	Gaia DR3 4070389125449668608	11.9	5.0	Symbiotic Star
7	PN Th 4-4	8.31	3.73	Gaia DR3 4119029875002043392	14.6	3.4	Symbiotic Star
8	PN M 2-9	10.90	18.06	Gaia DR3 4335188603873318656	13.9	1.3	Symbiotic Star
9	PN K 3-9	23.91	-1.54	Gaia DR3 4155672680486693120	15.3	2.6	Symbiotic Star
10	PN Ap 3-1	37.64	-2.97	Gaia DR3 4268140453591785984	14.3	3.9	Symbiotic Star
11	PN M 4-16	61.79	2.11	Gaia DR3 2022052808961769088	16.6	1.3	Symbiotic Star
12	Hen 2-468	75.94	-4.44	Gaia DR3 1870194997404105856	12.6	2.8	Symbiotic Star
13	PN M 1-2	133.12	-8.64	Gaia DR3 360112911622101120	12.6	1.2	Symbiotic Star
14	Hen 2-34	274.19	2.58	Gaia DR3 5409069172514684416	14.7	2.7	Symbiotic Star
15	Hen 2-25	275.22	-3.71	Gaia DR3 5310613021532357632	14.7	0.8	Symbiotic Star
16	Hen 2-106	312.03	-2.03	Gaia DR3 5853777267581362176	13.3	0.8	Symbiotic Star
17	Hen 2-104	315.48	9.46	Gaia DR3 6089564718596906880	13.6	0.8	Symbiotic Star
18	Hen 2-134	319.22	-9.35	Gaia DR3 5822400362454690688	12.1	2.5	Symbiotic Star
19	Hen 2-127	325.54	4.18	Gaia DR3 5889726659221998592	14.5	2.4	Symbiotic Star
20	PN Cn 1-2	326.41	-10.94	Gaia DR3 5818044445302448000	10.6	1.8	Symbiotic Star
21	PN Cn 1-1	330.78	4.15	Gaia DR3 5982979264021123968	10.8	1.1	Symbiotic Star
22	Hen 2-156	338.94	5.36	Gaia DR3 5992529686406981248	12.4	2.1	Symbiotic Star
23	Hen 2-176	339.39	0.74	Gaia DR3 5943382139466094720	13.6	4.1	Symbiotic Star
24	Hen 2-171	346.03	8.55	Gaia DR3 6020686328090453888	14.9	5.5	Symbiotic Star
25	PN H 2-4	352.95	3.93	Gaia DR3 5979902864926562176	14.2	3.2	Symbiotic Star
26	PN M 2-24	356.99	-5.80	Gaia DR3 4042147516455759744	15.1	0.8	Symbiotic Star
27	PN Th 3-20	357.41	2.62	Gaia DR3 4058701527427641472	14.0	2.8	Symbiotic Star
28	PN K 4-26	37.18	-6.85	Gaia DR3 4263728319553777408	13.9	6.7	Mira Variable Candidate
29	PN K 4-36	44.44	-10.38	Gaia DR3 4290522180961855872	12.7	4.7	M star
30	CD-48 6027	283.90	9.73	Gaia DR3 5362804330246457344	12.1	-0.3	Hot Subdwarf
31	Hen 2-58	289.18	-0.70	Gaia DR3 5338220285385672064	7.3	0.9	Wolf-Rayet

previously thought to be PNe. It is worth noting that all SySts in Table 2 are red in color.

3.2. Radial Velocity of PN CSs

The pioneering work for determining the RV of PNe was given by Schneider & Terzian (1983) who published the heliocentric RVs for 524 PNe. The next compilation (867 PNe) was reported by Durand et al. (1998). Beaulieu et al. (1999) reported the RVs of 45 PNe lying in the southern galactic bulge. Based on high dispersion spectra, Richer et al. (2017) reported the RVs of 76 PNe. Numerous other individual RVs are scattered throughout the literature (e.g., Ali et al. 2016; Ali & Dopita 2017, 2019). All the above measurements were derived from the Doppler shift of the nebular spectra. The Gaia mission opened a new window for calculating the RVs from the spectra of observed CSs. The Gaia RV was found by measuring the Doppler shift of a template spectrum and then comparing it to the spectrum that was seen.

Using the current release, we were able to detect the RVs for 51 PNe, including updated values for 14 PNe recorded by

Ali et al. (2022). Table 3 lists the newly detected RVs by Gaia DR3 and those obtained by Durand et al. (1998). The estimated median uncertainty of this compilation is 12.2%. In Figure 1, we compared the new RV measurements with those given by Durand et al. (1998). The diagonal line indicates the 1:1 matches. In general, the RVs computed from the spectra of both the CSs (Gaia DR3) and their associated nebulae are in good agreement. However, there are a few outliers related to high-velocity objects, such as H 2-24, SB 15, and Th 3-14. At first glance, all outlier objects have galactic longitudes of 0° – 10° or 350° – 360° , and galactic latitudes of 0° to $\pm 10^\circ$, indicating that they are located in the direction of the galactic bulge. To figure out the cause of this discrepancy, we examined the possible physical reasons, such as the interaction between PNe and the interstellar medium (ISM), the effect of nebular electron density, and the accuracy of RV measurements deduced from PNe and CSs. We found that none of these nebulae interact with the ISM, and the available electron density data for these objects did not provide a reasonable explanation. In addition, the accuracy of RV measurements

Table 3
The CS Radial Velocity of PNe in Gaia DR3

#	PN Name	Galactic Coordinate		RV (km s ⁻¹)		rv_nb_transits	rv_visibility_periods_used
		l	b	Gaia DR3	Durand et al. (1998)		
1	MPA J1803-3043	0.4	-4.22	-130.5 ± 6.0		3	2
2	Ap 1-11	3.12	-4.63	62.0 ± 3.9		4	4
3	H 2-24	4.33	1.84	28.0 ± 3.8	-198.2 ± 4.1	6	3
4	M 1-44	4.97	-4.96	-5.9 ± 0.5	-75 ± 11	4	4
5	SB 15	9.3	-6.53	-16.5 ± 4.7	165 ± 15	5	4
6	PN G009.8-07.5	9.87	-7.56	-23.3 ± 1.1	-32 ± 30	2	2
7	PN V-V 3-4	13.45	-4.25	-16.3 ± 4.7		7	7
8	UCAC4 374-117003	15.54	0.34	21.3 ± 2.2		8	8
9	SS 318	17.02	11.1	-36.7 ± 2.4		19	11
10	K 2-7	19.41	-19.66	-18.4 ± 0.5		14	12
11	PN G019.5-04.9	19.53	-4.96	-20.9 ± 1.4		13	9
12	Pe 1-15	25.91	-2.18	37.7 ± 3.7		6	4
13	IPHASX J191716.4+033447	39.08	-4.1	-4.2 ± 8.6:		9	9
14	K 1-14	45.61	24.32	-19.0 ± 1.0		63	22
15	VSP 2-30	49.32	2.38	-13.4 ± 1.9		27	18
16	Me 1-1	52.54	-2.96	-1.5 ± 11.4:	-6 ± 7	10	8
17	NGC 7008	93.41	5.49	-71.9 ± 7.7	-75.7 ± 2.7	18	11
18	IRAS 21282+5050	93.99	-0.12	28.2 ± 7.3		20	15
19	K 1-6	107.04	21.38	-55.7 ± 13.7		13	13
20	A 82	114.07	-4.67	-38.4 ± 2.3	-30.5 ± 3.3	23	16
21	PN M 1-2	133.12	-8.63	-28.4 ± 8.5	-12.1 ± 2	13	11
22	WeBo 1	135.67	1	-25.4 ± 4.6		33	17
23	NGC 1514	165.53	-15.29	42.3 ± 1.3	59.8 ± 4.4	21	10
24	H 3-75	193.65	-9.58	11.6 ± 2.6	22.9 ± 2	26	11
25	NGC 2346	215.7	3.62	31.5 ± 3.0	21.8 ± 0.9	13	10
26	PHR j0701-0749	221	-1.41	44.9 ± 2.9		14	11
27	LoTr 1	228.21	-22.14	15.8 ± 19.5:		31	19
28	PN V-V 1-7	235.44	1.89	38.9 ± 0.7		27	17
29	WRAY 15-158	255.33	-3.64	24.4 ± 2.3		22	19
30	LoTr 3	265.11	-4.21	16.2 ± 5.5	49 ± 3	19	15
31	NGC 3132	272.11	12.4	-11.1 ± 1.6	-16 ± 4.1	18	13
32	Hen 2-36	279.61	-3.19	-0.1 ± 1.5:	-7.1 ± 2	18	10
33	Hen 2-51	288.88	-5.22	13.5 ± 3.9	8 ± 3	13	12
34	Al 1	291.1	-39.66	1.1 ± 2.3:		16	15
35	Hen 2-70	293.61	1.2	64.6 ± 4.8		14	13
36	PN A66 35	303.57	40	-38.1 ± 4.6	-6.6 ± 3.8	9	8
37	SuWt 2	311.05	2.48	-15.7 ± 7.5	-40 ± 9	17	11
38	MPA J1508-6455	316.77	-5.8	-39.2 ± 11.9		43	17
39	Hen 2-134	319.22	-9.35	9.0 ± 0.7		45	21
40	PM 1-89	324.09	3.53	-68.5 ± 3.0	-81 ± 20	13	12
41	Hen 3-1312 (Sast 2-12)	334.84	-7.46	-70.6 ± 1.0	-77 ± -7	25	13
42	LoTr 5	339.89	88.46	-8.3 ± 1.7		21	13
43	Vd 1-1	344.27	4.75	-70.6 ± 1.0	-142.1 ± 2.5	11	10
44	SB 38	352.8	-8.41	-35.0 ± 7.0	59 ± 15	9	6
45	PHR J1711-3210	353.28	4.25	27.2 ± 1.7		10	6
46	PN G354.8+01.6	354.89	1.63	13.6 ± 6.6		13	10
47	Pe 1-11	358.01	-5.16	-11.9 ± 0.2	-130.6 ± 14	12	5
48	M 3-8	358.24	4.29	101.7 ± 3.4	95 ± 11	7	4
49	PHR J1752-3116	358.77	-2.5	-21.7 ± 8.4		2	1
50	Hen 3-1863	359.28	-33.5	4.3 ± 10.2:		19	14
51	Th 3-14	359.3	4.76	26.2 ± 20.4:	-239.2 ± 14	7	5

Note. The symbol (:) in column 4 refers to the RV measurement with high uncertainty.

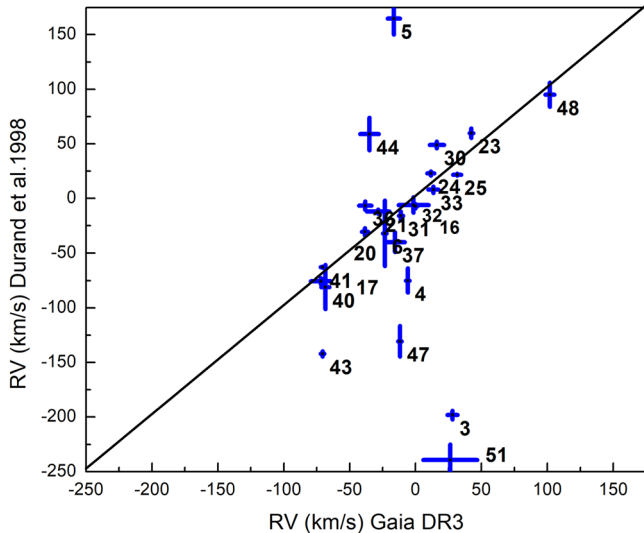


Figure 1. The RVs derived from the Gaia DR3 against those reported by Durand et al. (1998). The diagonal line refers to the 1:1 correlation. The numbers on the plot correspond to the PN numbers that are listed in Table 3.

derived from nebular emission lines is suitable. Thus, we examined the parameters that Gaia used to calculate the RV. We extracted two additional parameters relevant to the Gaia RV calculations: `rv_nb_transits` (the number of transits used to calculate the RV) and `rv_visibility_periods_used` (the number of visibility periods used to estimate the RV). Table 3 displays the previous two parameter values in columns 6 and 7. The preceding two parameters show that these outliers have a lower number of transits and shorter visibility periods compared with other RV measurements in Table 3. As a result, we may infer that the difference in RV measurements between the Gaia and nebular lines for these outlier objects is due to Gaia's inaccurate RV measurements.

4. Conclusions

We have discovered 82 PNe associated with CB CS candidates. To our knowledge, 58 members of this group have been found for the first time. This group of CB CSs comprises roughly half of all objects known in the literature. We also discovered photometric variability in 26 SySts and four stars of different types. Moreover, we detected the RVs of 51 PNe, 27 of which were identified for the first time. With a few exceptions, there is good agreement between the RVs measured from the absorption lines of the CSs and those measured from the emission lines of the PNe. In future work, we plan to extract the available photometric variability identifiers from the Gaia DR3 database to build the light curves for some of the objects mentioned in Table 1. We also plan to use the 74 inch telescope at the Kottamia Astronomical Observatory, Egypt, to perform a time-series photometric study for a few of the detected CB CS

candidates. Simultaneously, we will search the TESS and Kepler sky surveys, as well as the Optical Gravitational Lensing Experiment (OGLE) variable star catalog, for data that will allow us to confirm the binarity of the newly detected objects.

Acknowledgments

The authors would like to thank the reviewer for his or her constructive suggestions that helped enhance the original manuscript. This work has made use of data from the European Space Agency (ESA) mission Gaia (<https://www.cosmos.esa.int/gaia>), processed by the Gaia Data Processing and Analysis Consortium (DPAC, <https://www.cosmos.esa.int/web/gaia/dpac/consortium>). Funding for the DPAC has been provided by national institutions, in particular the institutions participating in the Gaia Multilateral Agreement.

ORCID iDs

A. Ali  <https://orcid.org/0000-0003-4180-8420>

References

- Afşar, M., & Ibanoglu, C. 2008, *MNRAS*, **391**, 802
 Ali, A., Algarni, E., Mindil, A., & Alghamdi, S. A. 2022, *RAA*, **22**, 085013
 Ali, A., & Dopita, M. A. 2017, *PASA*, **34**, e036
 Ali, A., & Dopita, M. A. 2019, *MNRAS*, **484**, 3251
 Ali, A., Dopita, M. A., Basurah, H. M., et al. 2016, *MNRAS*, **462**, 1393
 Aller, A., Lillo-Box, J., Jones, D., Miranda, L. F., & Barceló Forzeza, S. 2020, *A&A*, **635**, A128
 Beaulieu, S. F., Dopita, M. A., & Freeman, K. C. 1999, *ApJ*, **515**, 610
 Boffin, H. M. J., & Jones, D. 2019, *The Importance of Binaries in the Formation and Evolution of Planetary Nebulae* (Berlin: Springer)
 Chornay, N., Walton, N. A., Jones, D., et al. 2021, *A&A*, **648**, A95
 Ciardullo, R., Bond, H. E., Sipior, M. S., et al. 1999, *AJ*, **118**, 488
 Corradi, R. L. M., García-Rojas, J., Jones, D., & Rodríguez-Gil, P. 2015, *ApJ*, **803**, 99
 Creevey, O. L., Sordo, R., Pailler, F., et al. 2022, arXiv:2206.05864
 Cropper, M., Katz, D., Sartoretti, P., et al. 2018, *A&A*, **616**, A5
 De Angeli, F., Weiler, M., Montegriffo, P., et al. 2022, arXiv:2206.06143
 De Marco, O., Passy, J.-C., Frew, D. J., Moe, M., & Jacoby, G. H. 2013, *MNRAS*, **428**, 2118
 Douchin, D., De Marco, O., Frew, D. J., et al. 2015, *MNRAS*, **448**, 3132
 Durand, S., Acker, A., & Zijlstra, A. 1998, *A&AS*, **132**, 13
 Exter, K. M., Pollacco, D. L., & Bell, S. A. 2003, *MNRAS*, **341**, 1349
 Eyer, L., Audard, M., Holl, B., et al. 2022, arXiv:2206.06416
 Hillwig, T. C., Bond, H. E., Frew, D. J., Schaub, S. C., & Bodman, E. H. L. 2016, *AJ*, **152**, 34
 Ilkiewicz, K., & Mikołajewska, J. 2017, *A&A*, **606**, A110
 Jacoby, G. H., Hillwig, T. C., Jones, D., et al. 2021, *MNRAS*, **506**, 5223
 Jones, D., Lloyd, M., Santander-García, M., et al. 2010, *MNRAS*, **408**, 2312
 Katz, D., Sartoretti, P., Guerrier, A., et al. 2022, arXiv:2206.05902
 Miszalski, B., Acker, A., Moffat, A. F. J., Parker, Q. A., & Udalski, A. 2009, *A&A*, **496**, 813
 Miszalski, B., Corradi, R. L. M., Boffin, H. M. J., et al. 2011a, *MNRAS*, **413**, 1264
 Miszalski, B., Jones, D., Rodríguez-Gil, P., et al. 2011b, *A&A*, **531**, A158
 Munday, J., Jones, D., García-Rojas, J., et al. 2020, *MNRAS*, **498**, 6005
 Parker, Q. A., Bojičić, I. S., & Frew, D. J. 2016, *JPhCS*, **728**, 032008
 Pollacco, D. L., & Bell, S. A. 1994, *MNRAS*, **267**, 452
 Richer, M. G., Suárez, G., López, J. A., & García Díaz, M. T. 2017, *AJ*, **153**, 140
 Schneider, S. E., & Terzian, Y. 1983, *ApJL*, **274**, L61
 Wesson, R., Jones, D., García-Rojas, J., Boffin, H. M. J., & Corradi, R. L. M. 2018, *MNRAS*, **480**, 4589